Schlodder, E., & Brettel, K. (1988) *Biochim. Biophys. Acta 933*, 22-34.
Schlodder, E., & Brettel, K. (1990) in *Current Research in Photosynthesis* (Baltscheffsky, M., Ed.) Vol. I, pp 447-450, Kluwer, Dordrecht.
Seibert, M., Picorel, R., Rubin, A. B., & Connolly, J. S. (1988) *Plant. Physiol. 87*, 303-306.
Shipton, C. A., & Barber, J. (1991) *Proc. Natl. Acad. Sci. U.S.A.* (in press).
Takahashi, Y., Hansson, Ö., Mathis, P., & Satoh, K. (1987) *Biochim. Biophys. Acta 893*, 49-59.
Tetenkin, V. L., Gulyaev, B. A., Seibert, M., & Rubin, A. B. (1989) *FEBS Lett. 250*, 459-463.
Trebst, A. (1986) *Z. Naturforsch. 41c*, 240-245.
Treutlein, H., Schulten, K., Niedermeier, C., Deisenhofer, J., Michel, H., & DeVault, D. (1988) in *The Purple Bacterial Reaction Center: Structure and Dynamics* (Breton, J., & Verméglio, A., Eds.) pp 369-377, Plenum Press, New York.
Wasielewski, M. R., Johnson, D. G., Govindjee, Preston, C., & Seibert, M. (1989a) *Photosynth. Res. 22*, 89-99.
Wasielewski, M. R., Johnson, D. G., Seibert, M., & Govindjee (1989b) *Proc. Natl. Acad. Sci. U.S.A. 86*, 524-528.
Webber, A. N., Packman, L., Chapman, D. J., Barber, J., & Gray, J. C. (1989) *FEBS Lett. 242*, 259-262.
Woodbury, N. W. T., & Parson, W. W. (1984) *Biochim. Biophys. Acta 767*, 345-361.

Photoinhibition of Hydroxylamine-Extracted Photosystem II Membranes: Identification of the Sites of Photodamage†

Danny J. Blubaugh,‡,§ Mike Atamian,∥ Gerald T. Babcock,∥ John H. Golbeck,⊥ and George M. Cheniae*,‡
University of Kentucky, Lexington, Kentucky 40546-0091, Department of Chemistry, Michigan State University, East Lansing, Michigan 48824, and Department of Biochemistry, University of Nebraska, Lincoln, Nebraska 68583-0718
Received December 28, 1990; Revised Manuscript Received May 8, 1991

ABSTRACT: Electron paramagnetic resonance (EPR) analyses ($g = 2$ region) and optical spectrophotometric analyses of P_{680}^+ were made of NH_2OH-extracted photosystem II (PSII) membranes after various durations of weak-light photoinhibition, in order to identify the sites of damage responsible for the observed kinetic components of the loss of electron transport [Blubaugh, D. J., & Cheniae, G. M. (1990) *Biochemistry 29*, 5109-5118]. The EPR spectra, recorded in the presence of $K_3Fe(CN)_6$, gave evidence for rapid ($t_{1/2}$ = 2-3 min) and slow ($t_{1/2}$ = 3-4 h) losses of formation of the tyrosyl radicals Y_Z^+ and Y_D^+, respectively, and the rapid appearance ($t_{1/2}$ = 0.8 min) of a 12-G-wide signal, centered at $g = 2.004$, which persisted at 4 °C in subsequent darkness in rather constant abundance ($\sim^1/_2$ spin per PSII). This latter EPR signal is correlated with quenching of the variable chlorophyll *a* fluorescence yield and is tentatively attributed to a carotenoid (Car) cation. Exogenous reductants ($NH_2OH \geq NH_2NH_2 > DPC \gg Mn^{2+}$) were observed to reduce the quencher, but did not reverse other photoinhibition effects. An additional 10-G-wide signal, tentatively attributed to a chlorophyll (Chl) cation, is observed during illumination of photoinhibited membranes and rapidly decays following illumination. The amplitude of formation of the oxidized primary electron donor, P_{680}^+, was unaffected throughout 120 min of photoinhibition, indicating no impairment of charge separation from P_{680}, via pheophytin (Pheo), to the first stable electron acceptor, Q_A. However, a 4-μs decay of P_{680}^+, reflecting $Y_Z \rightarrow P_{680}^+$, was rapidly ($t_{1/2}$ = 0.8 min) replaced by an 80-140-μs decay, presumably reflecting Q_A^-/P_{680}^+ back-reaction. Photoinhibition caused no discernible decoupling of the antenna chlorophyll from the reaction center complex. We conclude that the order of susceptibility of PSII components to photodamage when O_2 evolution is impaired is $Chl/Car > Y_Z > Y_D \gg P_{680}$, Pheo, Q_A.

Photosystem II (PSII)[1] is a large membrane-bound multiprotein complex that photochemically catalyzes the oxidation of water and the reduction of plastoquinone. Its reaction center (RC) consists of a heterodimer of homologous polypeptides, D_1 and D_2, which together contain the primary electron donor chlorophyll(s) (P_{680}), the secondary electron donor tyrosines Y_Z and Y_D of D_1 and D_2, respectively, the intermediate electron acceptor to P_{680}, pheophytin (Pheo), and the primary (Q_A) and secondary (Q_B) plastoquinone electron acceptors, along with an associated non-heme Fe. Closely associated with the RC is cyt *b*-559, the function of which is not clear. Light

† This work was supported principally by the U.S. Department of Energy (Contract DE-FG05-86ER13533 to G.M.C.) and partially by the USDA Competitive Research Grants Office, Photosynthesis Program (90-37262-5701 to G.T.B.), and the National Science Foundation (NSF DMB-8905065 to J.H.G.). A portion of this work was presented at the VIIIth International Congress on Photosynthesis (Blubaugh & Cheniae, 1990a). This paper (91-32) is published with approval of the Kentucky Agricultural Experiment Station.
* To whom correspondence should be addressed.
‡ University of Kentucky.
§ Present address: Department of Chemistry and Biochemistry, Utah State University, Logan, UT 84322-0300.
∥ Michigan State University.
⊥ University of Nebraska.

[1] Abbreviations: C_1^+ and C_2^+, photooxidizable radicals, tentatively associated with Chl^+ and Car^+, respectively; Car, carotenoid; Chl, chlorophyll; cyt *b*-559, cytochrome *b*-559; D_1 and D_2, homologous 32-kDa polypeptides which, as a dimer, form the PSII RC core; DCIP, 2,6-dichlorophenolindophenol; DCMU, 3-(3,4-dichlorophenyl)-1,1-dimethylurea; DPC, diphenylcarbazide; EPR, electron paramagnetic resonance; MES, 2-(*N*-morpholino)ethanesulfonic acid; NH_2OH-PSII, PSII membranes extracted with NH_2OH to inactivate water oxidation; P_{680}, PSII primary electron donor chlorophyll; Pheo, pheophytin; PSII, photosystem II; Q_A and Q_B, primary and secondary plastoquinone electron acceptors of PSII, respectively; RC, reaction center; S_n (state), oxidation state of the WOC; WOC, water-oxidizing complex; Y_Z and Y_D, redox-active tyrosines-161 and -160, respectively, of the D_1 and D_2 RC polypeptides.

0006-2960/91/0430-7586$02.50/0

absorption produces a transient charge separation (P_{680}^+/Pheo$^-$), which is rapidly stabilized by the reduction of P_{680}^+ by Y_Z (20 ns–20 μs, dependent on the pH and the state of the WOC) and the oxidation of Pheo$^-$ by Q_A (300–600 ps), which in turn is oxidized (200–400 μs) by Q_B. At the Q_B site, reduced plastoquinol exchanges for another plastoquinone. In oxygen-evolving systems, the Y_Z^+ formed is rapidly reduced ($\leq$1 ms) by the tetra-Mn oxygen-evolving complex, which cycles through a series of oxidation states, S_n, where n = 0–4. [For reviews of PSII, see Mathis and Rutherford (1987), Babcock (1987), Babcock et al. (1989), and Hansson and Wydrzynski (1990).]

Exposure of oxygenic photosynthetic organisms to light intensities higher than those to which they are adapted leads to an inhibition of O_2 evolution, of electron-transfer reactions, and of CO_2 fixation, as a consequence of photodamage to PSII [for reviews, see Powles (1984) and Kyle (1987)]. In addition, photoinhibition promotes the disassembly of the PSII complex: (1) the inherently high light-dependent rate of D_1 degradation (and to a lesser extent the D_2), which occurs in vivo under normal light conditions (Matoo et al., 1984), is accelerated (Ohad et al., 1984; Hundal et al., 1990b; Virgin et al., 1990); (2) the 33-, 23-, and 16-kDa extrinsic proteins associated with O_2 evolution, as well as the Mn complex, become dissociated (Virgin et al., 1988; Hundal et al., 1990a); and (3) the intrinsic PSII polypeptides move laterally from appressed to nonappressed regions of the thylakoid membrane (Hundal et al., 1990a). Presumably, similar disassembly occurs following weak-light photoinhibition of photosynthetic cells made unable to evolve O_2 prior to photoinhibition (Callahan & Cheniae, 1985). Such events may reflect oxidation or modification of specific amino acid residues of the D_1 (Kyle, 1987; Adir et al., 1990) or both the D_1 and D_2 polypeptides (Callahan et al., 1986). This inhibits specific forward electron-transfer reactions and promotes the proteolysis of the heterodimer RC polypeptide(s). Restoration of PSII activity then requires synthesis and assembly of the RC polypeptide(s) (Ohad et al., 1984; Callahan et al., 1986; Becker et al., 1987; Adir et al., 1990), their reassociation with the extrinsic polypeptides, and the reassembly of the Mn complex (Becker et al., 1985; Ono et al., 1986). Alternatively, independent of protein synthesis, recovery from photoinhibition may occur by lateral migration of nonphotoinhibited PSII β-centers from nonappressed to appressed lamellae to become O_2-evolving, Q_β-reducing PSII α-centers (Neale & Melis, 1990; Hundal et al., 1990b).

Appreciable efforts have been made by different laboratories to identify the first electron-transfer reaction affected during photoinhibition. These studies have led to differing hypotheses for the reactions triggering protein damage. One hypothesis holds that damage occurs at the Q_B site from accumulation of radical species of O_2 (Kyle et al., 1984; Kyle, 1987) or that destabilization of Q_B^- binding occurs, followed by an irreversible modification of D_1 (Ohad et al., 1988, 1990). Occupancy of the Q_B site has been suggested to mediate these reactions (Critchley, 1988; Trebst et al., 1990).

Other workers advocate that initial damage occurs either at the primary P_{680}^+/Pheo$^-$ charge separation (Cleland et al., 1986; Demeter et al., 1987; Neale & Melis, 1990) or at Q_A (Allakhverdief et al., 1987; Vass et al., 1988; Styring et al., 1990). The acceleration of photoinhibition by strict anaerobiosis (Trebst, 1962; Satoh & Fork, 1982; Krause et al., 1985; Arntz & Trebst, 1986), which promotes reduction of Q_A and Q_B during illumination, tends to support the above conclusions obtained from nonstressed oxygenic cells and cell-free preparations.

Separate hypotheses have arisen from studies with higher plant PSII preparations pretreated to inhibit the water-oxidizing reactions (Callahan et al., 1986; Theg et al., 1986; Jegerschold et al., 1990; Blubaugh & Cheniae, 1990b; Klimov et al., 1990) or with *Synechocystis* subjected to stresses impairing water oxidation (Zhao & Brand, 1988, 1989). Under such conditions, the lifetimes of Y_Z^+ and P_{680}^+, as well as S_2 and S_3 (in instances of Cl^- and Ca^{2+} depletion, respectively), are prolonged. Consequently, on illumination of PSII, the nearby pigments and polypeptides comprising the PSII RC and those providing ligands for the Mn^{2+}, Ca^{2+}, and Cl^- of the WOC are subject to exposure to very high redox potentials, and the susceptibility of PSII to photodamage increases as much as ~400-fold relative to oxygenic PSII systems.

The studies made with higher plant PSII preparations having inhibited or inactive WOC's indicate that irreversible photodamage occurs first to the oxidizing side of PSII as determined by specific loss of O_2-evolving activity following (1) photoinhibition of Cl^--depleted chloroplasts, then Cl^- readdition before assays (Theg et al., 1986; Jegerschold et al., 1990), and (2) photoinhibition of Mn-less preparations and subsequent photoactivation of the WOC before assays (Callahan & Cheniae, 1985; Klimov et al., 1990; Blubaugh & Cheniae, 1990b). In all these studies, a loss of PSII photooxidation of exogenous donors is subsequently observed and, additionally, a parallel degradation of D_1 (Jegerschold et al., 1990). These latter events, also resulting from photodamage to the oxidizing side of PSII, have been postulated to reflect a second oxidation of P_{680}^+ (Theg et al., 1986) or a second oxidation of Y_Z^+ (Callahan et al., 1986) or photodamage to an electron carrier outside of the Y_Z, Y_D, P_{680}, and Q_A section of the PSII RC (Klimov et al., 1990). Weak-light photoinhibition of *Synechocystis* in a Na^+-free medium results in a similar pattern of photodamage. An inactivation of the WOC (reversed by Na^+ addition) is followed immediately by a disconnection of PSII antenna chlorophyll (reversed only by protein synthesis) and then photodamage to the PSII RC (Zhao & Brand, 1988, 1989).

The high susceptibility of non-O_2-evolving PSII complexes to photoinhibition and the severe limitations this imposes on the photoactivation of O_2 evolution prompted the work reported here. This work is an outgrowth from a previous report (Blubaugh & Cheniae, 1990b), which gave evidence for three kinetically distinguishable sites of photodamage occurring with approximate half-times of 0.8 min, 2–3 min, and 1–4 h. The latter two components were attributed to photodamage affecting Y_Z^+ and possibly Y_D^+ formation, respectively; however, these assignments were made from somewhat indirect arguments, and no assignment could be made to the 0.8-min component that affected photoactivation and the amplitude of variable Chl *a* fluorescence. In efforts to definitively describe the loci of photodamage resulting from photoinhibition of NH_2OH-treated PSII membranes, EPR and optical measurements were made of the abundances of Y_Z^+, Y_D^+, P_{680}^+, and P_{680}^+ decay rates after various durations of photoinhibition. Additionally, analyses were made of a light-induced featureless 10–12-G-wide EPR signal (g = 2.0024) (Visser & Rijgersberg, 1975; Visser et al., 1977; de Paula et al., 1985), seen here at ambient temperature. This signal previously has been suggested to arise from C^+, a Chl cation radical (Visser et al., 1977), or possibly a carotenoid radical (Schenck et al., 1982). More recently, this radical has been postulated to arise by oxidation of a nearby Chl by P_{680}^+ in the first event of photoinhibition (Thompson & Brudvig, 1988). Our analyses (1) suggest the occurrence of two radicals, C_1^+ and C_2^+, with very

similar single-line EPR spectra of 10- and 12-G widths, respectively, but with different stabilities following photoinhibition, (2) permit unambiguous identification of the 0.8-min, 2–3-min, and 1–4-h kinetic components, respectively, with C_1^+/C_2^+ formation, loss of Y_Z, and loss of Y_D, and (3) exclude P_{680}, Pheo, and Q_A as sites of photodamage under our experimental conditions.

Materials and Methods

Sample Preparation. The preparation of wheat NH_2OH-extracted PSII membranes (NH_2OH-PSII), their subsequent photoinhibition by weak light (40 μE m^{-2} s^{-1} from cool-white fluorescent lamps), and the determination of their capacities for photoactivation and electron transport (DCIP photoreduction; O_2 evolution) have been described by Blubaugh and Cheniae (1990b). For most of the experiments reported here, the photoinhibition was done in batches of 11-mL volumes (250 μg of Chl/mL) in 600-mL beakers, with the sample thickness ~2 mm. Several such batches were pooled and then concentrated by centrifugation to 3–4 mg of Chl/mL. The samples were then stored at −80 °C. For the EPR measurements, the samples were used undiluted. For activity assays and the measurements of P_{680}^+ in Figure 5, the same samples were first diluted to ~240 μg of Chl/mL in 0.8 M sucrose, 50 mM MES, and 15 mM NaCl, pH 6.5 (buffer A), and homogenized, and the [Chl] was redetermined before further dilutions and analysis. In some experiments (Figures 6–9), the membranes were photoinhibited as described previously (Blubaugh & Cheniae, 1990b). Determinations of [Chl] were made as described by MacKinney (1941). All handling of membranes prior to and following photoinhibition was done in strict darkness.

EPR Measurements. Immediately prior to the EPR measurements, the thawed samples were supplemented (from 100× stock solutions) with, unless stated otherwise, 1 mM ferricyanide, 1 mM ferrocyanide, and 2 mM EDTA. The measurements were made at room temperature in standard quartz flat cells, with a Bruker ER-200D spectrometer operating near 9.5 GHz. A projection lamp provided illumination of 2.3 mE m^{-2} s^{-1} (white light) at the slotted face of the EPR cavity. The microwave power was 20 mW, with a modulation amplitude of 5.0 G. The first-derivative spectra were normalized with respect to [Chl] (values ranged from 3.0 to 3.7 mg/mL).

Chlorophyll a Fluorescence Yield and P_{680}^+ Formation and Decay. The procedure for measurements of flash-induced Chl *a* fluorescence yield has been described (Blubaugh & Cheniae, 1990b). The formation and decay of P_{680}^+ were measured at room temperature by recording the 820-nm absorbance changes induced by a 600-ps, 1.4 mJ N_2 laser pulse (PTI Model PL2300; λ = 337.1 nm) presented to samples (~80 μg of Chl/mL) suspended in buffer A containing 4 mM EDTA and, where indicated, 1 mM ferricyanide. A laser diode (Spindler & Hoyer Model DC25F) provided the monochromatic 820-nm measuring light, and a fast photodiode (UDT Model PIN 10D, reverse-biased to 15 V) coupled to a 70-MHz amplifier (EG & G Model 115) and digital signal averager (Tektronix Model DSA 601 with submicrosecond resolution) served as the detection system. The detecting photodiode was separated from the sample by 3 m to minimize fluorescence artifacts and interference by scattered actinic light. Signal averaging of 16 flashes at a frequency of 1 Hz was used on all samples. Data were normalized to [Chl].

Results

Effects of Photoinhibition on EPR Spectra. NH_2OH-PSII membranes that had been prepared in strict darkness were photoinhibited in weak light for 1–120 min, then concentrated, and stored at −80 °C for several months. After being thawed, the membranes were maintained on ice in strict darkness before the analyses by EPR (Figure 1). These analyses were done sequentially beginning with the t = 0 sample; consequently, the length of time at ~4 °C varied, increasing progressively up to ~8–10 h for the 120-min photoinhibited sample. Furthermore, because the photoinhibition was done in batches (Materials and Methods), the length of time at ~4 °C in the dark immediately after the photoinhibition, prior to concentration and freezing, also increased progressively. According to Buser et al. (1990), ~15% Y_D^+ remains after a >3-h dark-adaptation of NH_2OH-PSII following illumination; thus, because of the varying dark times at 4 °C, the amount of Y_D^+ remaining in the dark-adapted photoinhibited samples was not controlled.

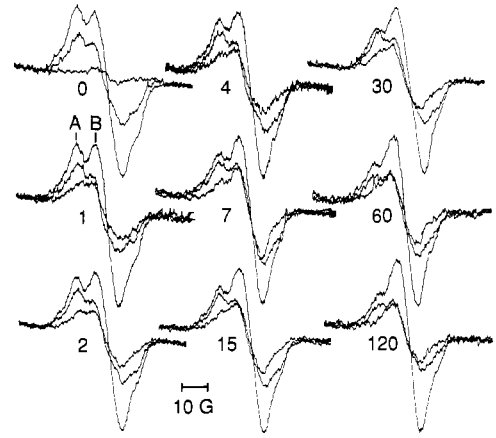

FIGURE 1: Room temperature EPR spectra (g = 2 region) from wheat NH_2OH-PSII after various durations of photoinhibition. The minutes of photoinhibition are indicated by the number next to each set of traces. In each set of three, the inner trace was obtained first in the dark, then the outer trace was obtained during 20 s of continuous illumination, and finally the middle trace was obtained in the dark 1 min after turning off the light; 1 mM ferrocyanide, 1 mM ferricyanide, and 2 mM EDTA were added to the membranes immediately prior to the measurements. Other experimental conditions are described under Materials and Methods. The "peaks" labeled A and B are the "low-field shoulder" and "low-field maximum", respectively. The "dark-after-light" spectra had zero-crossings between g = 2.0040 and 2.0046.

Three overlaid first-derivative spectra (g = 2 region) are shown in Figure 1 for each photoinhibited sample. In each set of three, the smallest spectrum (shown by the inner line) was recorded in strict darkness. The largest signals (outer line) in each set were recorded during 20 s of continuous illumination, while the intermediate-size signals were recorded in darkness 1 min after cessation of the illumination. With thoroughly dark-adapted Tris- or NH_2OH-extracted chloroplasts and PSII membranes, this assay regime normally shows no EPR signals in the initially recorded dark trace, approximately equal abundances of Y_Z^+ and Y_D^+ formed during continuous illumination, and then only the spectrum of Y_D^+ after a 1-min dark interval [the half-time for reduction of Y_Z^+ in NH_2OH-PSII membranes in the absence of exogenous reductants is ~40–50 ms (Dekker et al., 1984; Buser et al., 1990)]. The spectra shown in Figure 1 for nonphotoinhibited NH_2OH-PSII (t = 0) are entirely consistent with the many previous reports made with dark-adapted Tris- or NH_2OH-treated PSII preparations.

In a separate control experiment not shown, NH_2OH-PSII membranes went through identical handling procedures as the 120-min photoinhibited samples, except that there was no illumination. The resulting EPR spectra were identical in all

respects with those shown for the nonphotoinhibited (t = 0) spectra. Therefore, the effects of photoinhibition described below are due entirely to the illumination, and not to any of the handling or storage steps associated with the treatment.

A general comparison of the set of spectra shown in Figure 1 reveals the following: (1) the amplitude of the low-field maximum at B under continuous illumination was constant, irrespective of the duration of photoinhibition, whereas the amplitude of the low-field shoulder at A was progressively diminished; (2) in subsequent darkness, the amplitudes at both A and B were rather constant up to ~15 min of photoinhibition, whereas with >15-min photoinhibition, they became progressively less, with the low-field shoulder diminishing somewhat more rapidly; and (3) all of the photoinhibited samples showed signal(s) even without re-illumination, as a result of radical(s) formation during photoinhibition and incomplete decay before and during storage and subsequent EPR analyses. The ratio of the amplitudes of the initial dark-recorded low-field maxima to low-field shoulders was greater in samples photoinhibited for ≥30 min, but may simply indicate greater Y_D^+ reduction due to longer times at 4 °C/dark. These, and similar observations made with photoinhibited chloroplasts (unpublished data of Curt W. Hoganson, David W. Becker, and G.M.C.), indicate that photoinhibition of NH_2OH-PSII is a complex process causing a hierarchy of kinetically separable photodamaging effects on the reaction center components (Blubaugh & Cheniae, 1990b).

Over the course of 15 min, photoinhibition had little effect on the abundance of Y_D^+, since the amplitude of the low-field shoulder following continuous illumination and then 1-min darkness was invariant. Therefore, the decrease in the amplitude of the light-recorded low-field shoulder in ≤15-min-photoinhibited samples indicates a rapid loss of Y_Z^+ formation. This loss was substantial in only a few minutes of photoinhibition and was virtually complete in 15–30 min.

A second and much slower effect of photoinhibition is a decrease in the abundance of Y_D^+. Photoinhibition times >15 min gradually diminished the amplitude of the low-field shoulder observed after continuous illumination and short darkness; nevertheless, appreciable Y_D^+ was still observed even after 120 min of photoinhibition. Other features of the spectral changes are discussed in subsequent sections.

Photodamage affecting formation of Y_Z^+ and Y_D^+ could also be seen in real time during illumination of NH_2OH-PSII in the EPR cavity itself. In the experiment of Figure 2A, nonphotoinhibited NH_2OH-PSII membranes were illuminated continuously for >1 h in the absence of ferri/ferrocyanide while the amplitude of the Y_Z^+ and Y_D^+ signals at the low-field shoulder was recorded (g = 2.0109). In the absence of the electron acceptor, the light intensity was insufficient to initially fully generate Y_Z^+, presumably because the back-reaction between Y_Z^+/Q_A^- [$t_{1/2}$ ~40–50 ms (Dekker et al., 1984; Buser et al., 1990)] competed significantly with Y_Z oxidation by P_{680}^+ (limited by the rate of P_{680} turnover). Under such conditions, the continuous illumination yielded a "maximum" Y_Z^+/Y_D^+ signal which then diminished with clear biphasic kinetics. The fast-decaying component is attributed to photodamage affecting Y_Z^+ formation, and the ≥100 times slower decaying component is attributed to photodamage affecting Y_D^+ formation.

These assignments are reinforced by the results shown in Figure 2B–D. In these experiments, the membranes were continuously illuminated in the presence of ferri/ferrocyanide to permit maximum Y_Z^+/Y_D^+ formation. As shown in Figure 2B, the low-field shoulder in nonphotoinhibited (t = 0)

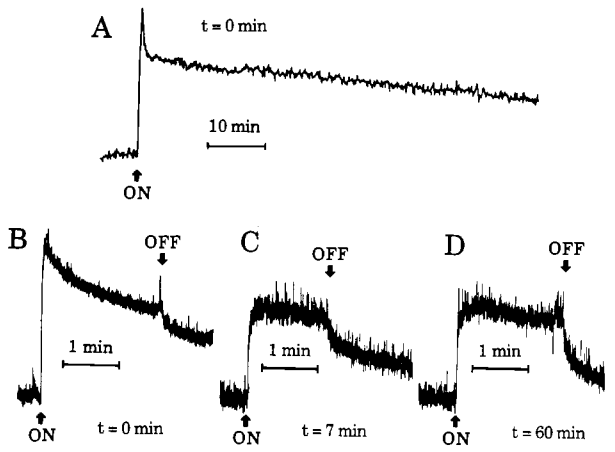

FIGURE 2: Time course of loss of the Y_Z^+ and Y_D^+ EPR signals in wheat NH_2OH-PSII, measured at the low-field shoulder (g = 2.0109; field position A in Figure 1), during continuous illumination of the EPR cell cavity. Illumination began and ended as indicated by the "on" and "off" arrows. The light intensity (white light) at the slotted face of the cell cavity was 2.3 mE m^{-2} s^{-1}. The membranes were previously photoinhibited (Materials and Methods) for (A, B) 0 min, (C) 7 min, or (D) 60 min. Experimental conditions were the same as in Figure 1, except that in (A) no ferri/ferrocyanide was present. The Chl concentration was 3–4 mg/mL. The gain in (C, D) was 1.6× that in (B).

NH_2OH-PSII declined exponentially to about 50% of its initial amplitude (most of the Y_Z^+ lost) after only ~2-min illumination. On the other hand, with membranes previously photoinhibited for either 7 min (Figure 2C) or 60 min (Figure 2D) to essentially abolish Y_Z^+ formation (Figures 1 and 2A), the initial signal amplitude was diminished compared to nonphotoinhibited NH_2OH-PSII (Figure 2B), and no substantial decrease in the signal occurred during the continuous illumination. Thus, the real-time analyses of effects of continuous illumination on Y_Z^+ and Y_D^+ formation confirm the conclusions reached from the data of Figure 1. In a later section, explanations are given for the rapid decay of the EPR signal(s) observed in Figure 2B–D on cessation of illumination.

Evidence for Chl$^+$ and Car$^+$ Formation during Photoinhibition. A prominent feature in the light-recorded EPR spectra, particularly of the ≥4-min photoinhibited samples in Figure 1, is the featureless signal with a peak-to-peak width of 10 G, centered at g = 2.003. This signal has a striking resemblance to a C^+ signal (identity unknown), previously observed at cryogenic temperatures, a condition which blocks electron transfer from Y_Z to P_{680}^+ (de Paula et al., 1985), and recently at room temperature in the presence of acetone hydrazone (Tso et al., 1990).

A similar signal is observed in the dark-recorded spectra (e.g., Figure 1, 120 min), but it is wider (~12 G) and shifted slightly downfield (g = 2.0042) in relation to the C^+ signal in the light-recorded spectra. It bears a resemblance to a 14-G signal observed in PSII treated with a high concentration of acetate, which slows $Y_Z \rightarrow P_{680}^+$ electron transfer (Bock et al., 1988). These spectral differences suggest two separate radical species, although we cannot exclude the possibility of a single species in somewhat different environments that affect stability. Evidence exists for both Chl (Visser et al., 1977) and Car (Schenck et al., 1982) oxidation when $Y_Z \rightarrow P_{680}^+$ is impaired. Furthermore, both cations have very similar single-line EPR spectra centered at $g \approx 2.003$ [ΔH_{pp} = 8 G for known Chl^+ radicals, such as P_{700}^+ and P_{680}^+; ΔH_{pp} ~ 14 G for Car^+ radicals in organic solvents (Grant et al., 1988)]. Car^+ radicals have also been shown to be quite stable at room temperature, with half-lives of several minutes, depending on

the solvent (Grant et al., 1988). From these considerations, we tentatively assign the light-recorded 10-G signal (C_1^+) to Chl^+ [see also Visser et al. (1977), de Paula et al. (1985), and Thompson and Brudvig (1988)] and the dark-stable 12-G signal (C_2^+) to Car^+. We cannot, however, rule out the possibility that either or both signals may represent a modified Y_Z^+ and/or Y_D^+, or a modified environment of the tyrosyl radical(s) as hypothesized by Tso et al. (1990) and Baumgarten et al. (1990).

The constancy of the low-field maximum in the light-recorded spectra of Figure 1 suggests that C_1^+ (Chl^+) is formed more readily as Y_Z^+ formation is lost and continues to be formed following subsequent decrease of Y_D^+ formation. We exclude possible contributions of P_{680}^+ to this signal, because in the absence of ferri/ferrocyanide the observable abundance of Y_Z^+, but not of C_1^+, was substantially reduced in non-photoinhibited membranes with the limiting light intensity employed (data not shown). The absence of a significant Y_Z^+ signal under such conditions suggests that the RC turnover rate was slower than the half-time of the Y_Z^+/Q_A^- back-reaction [$t_{1/2}$ ~40–50 ms (Dekker et al., 1984; Buser et al., 1990)] and thus far slower than the P_{680}^+/Q_A^- back-reaction [$t_{1/2}$ ~100 μs (Conjeaud & Mathis, 1980)]. Consequently, essentially no steady-state P_{680}^+ would be present at conditions clearly yielding the C_1^+ signal.

We also note the following: (1) in subsequent brief darkness, the Y_Z^+ and C_1^+ contributions to the low-field maximum decayed; (2) the 1–30-min photoinhibited membranes (but not the $t = 0$ control) gave initially dark-recorded spectra showing features of a mixed Y_D^+ and C_2^+ population (~$^1/_2$ spin per PSII), while the similarly recorded spectrum made with 60–120-min photoinhibited membranes gave evidence for essentially only C_2^+; and (3) full abundance of Y_D^+ and little C_2^+ remained after a 1-min dark period following the illumination of 60–120-min photoinhibited samples in the EPR cavity.

The first observation implies that C_1^+ decays rather rapidly. Support for this argument can be derived from the rapid dark decay of the signal(s) shown in Figure 2C–D. The traces of Figure 2C–D were obtained with the same 7- and 60-min photoinhibited samples, respectively, that in parallel experiments yielded the EPR spectra labeled 7 and 60 in Figure 1. In Figure 2C–D, however, we observe upon illumination a rapid and a slow rise in the signal (field position A), which can be attributed predominantly to C_1^+. Thus, the rising signal appears to be at least biphasic. Because of the longer duration of illumination in the experiments of Figure 2C–D (>1 min) relative to those of Figure 1 (≤10 s by the time field position A was measured), it is expected that the extent of C_1^+ formation would be greater in Figure 2C–D and, indeed, the extent of the dark decay upon cessation of illumination is greater in Figure 2C–D than in the corresponding samples in Figure 1. We note that the extent of the dark decay is similar between corresponding samples, if the amplitude of only the fast rising signal in Figure 2C–D is used as the basis of comparison.

The rapid dark decay of the signal(s) at field position A with photoinhibited membranes exhibiting extensive or complete loss of Y_Z^+ formation was previously attributed to an accelerated dark decay of Y_D^+ (Blubaugh & Cheniae, 1990a). Although this idea cannot be ruled out, our data are adequately explained by an overlap of the fast-decaying C_1^+ signal with the low-field shoulder of Y_D^+ at field position A [see spectra of Nugent et al. (1982) and de Paula et al. (1985)]. We conclude that C_1^+ is generated biphasically during sustained illumination (Figure 2C–D). Also, the faster and more extensive dark decay after 60 min (Figure 2D) versus 7 min (Figure 2C) of photoinhibition confirms the conclusion made from the data of Figure 1 that more C_1^+ is generated with longer duration of photoinhibition; its decay may also be accelerated.

Second, the mixed Y_D^+/C_2^+ (Car^+) signal observed in the initial dark spectra of the 1–60-min photoinhibited samples reflects their formations during the photoinhibition treatment and an incomplete decay during uncontrolled dark storage and handling of samples prior to EPR analyses. Little, if any, Y_D^+ was present in the initial dark spectrum of the 120-min sample, which received longer dark incubation at 4 °C before EPR analyses than the other samples (see previous section). Apparently, the stability of $C_2^+ > Y_D^+$.

Finally, to explain observation 3, we suggest that C_2^+ is oxidized to the dication form (Car^{2+}) during illumination. The dication would be EPR-silent, but upon subsequent dark storage, a slow reaction of C_2^{2+} to form C_2^+ would regenerate the dark-stable EPR signal. β-Carotene in some organic solvents is known to readily undergo a two-electron oxidation; a monovalent cation is also produced, presumably by reaction of the dication with a neutral β-carotene molecule (Grant et al., 1988). We cannot rule out other possibilities, such as (1) a rapid Q_A^-/C_2^+ charge recombination during illumination and a slow oxidation of C_2 by Y_D^+ during long dark storage [as occurs with cyt *b*-559 (Vass et al., 1990)], or (2) stability of C_2^+ after prolonged but not after short illumination periods, due to a progressive oxidation of Q_A^- during long illuminations in the absence of any electron donors. However, formation of the dication is more consistent with the analyses that follow.

Quantitation of the Rates of C_1^+/C_2^+ Formation and Loss of Y_Z^+/Y_D^+ Formation. The loss of electron donor photooxidations during photoinhibition revealed two first-order kinetic components with half-times of 2–3 min and 1–4 h (Blubaugh & Cheniae, 1990b). Additionally, another component ($t_{1/2}$ ~0.8 min) was reported which correlated with a loss of ~50% of the capacity for photoactivation and a large (>60%) quenching of the flash-induced variable Chl *a* fluorescence. These effects could be generally assigned to photodamage to the oxidizing side of PSII; however, only the assignment of Y_Z to the 2–3-min component could be made with much confidence. Thus, we used the same control and photoinhibited membranes used in the experiments of Figures 1 and 2 (and Figure 5) and reanalyzed the kinetics of losses of photoactivation and Mn^{2+} and DPC photooxidations according to the methods of Blubaugh and Cheniae (1990b). Best fits of the data to multicomponent exponential decays gave half-times of 0.6–0.9, 2.3, and 204–264 min (data not shown), values very similar to those previously reported. We then analyzed the data of Figure 1 to obtain the kinetics of loss of Y_Z^+ and Y_D^+ and the kinetics of C_1^+ and C_2^+ formation in attempts to correlate their changes during photoinhibition with the above half-times.

A quantitative analysis of the rates of loss of Y_Z^+ and Y_D^+ proved complicated because of the overlap of the tails of the C_1^+ and C_2^+ signals with the Y_Z^+ and Y_D^+ signals at the low-field shoulder ($g = 2.0109$). As a first approximation, however, we ignored the C_1^+ and C_2^+ tails and plotted the relative amplitudes of the Y_Z^+ and Y_D^+ amplitudes at $g = 2.0109$ versus time of photoinhibition. Panels A and B of Figure 3 show the analyses for Y_Z^+ and Y_D^+, respectively. The solid lines shown in Figure 3A,B are calculated single-exponential decay-curves having half-times of 2.87 and 168 min, respectively. A reasonably good fit between the data points and the calculated curves is observed with the exception of the

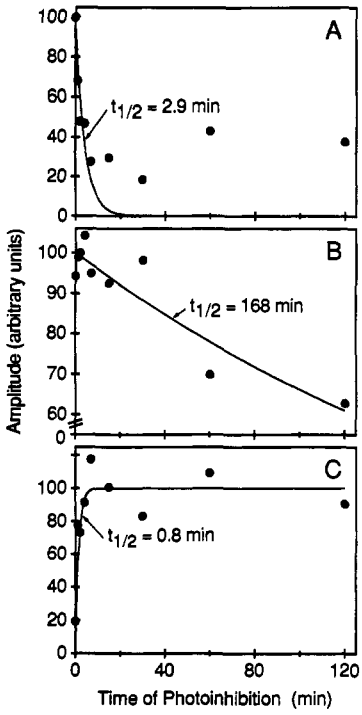

FIGURE 3: Analysis of the rates of (A) loss of Y_Z^+ formation, (B) loss of Y_D^+ formation, and (C) appearance of stable C_2^+ during photoinhibition of wheat NH_2OH-PSII. The data are from the EPR spectra of Figure 1. Plotted in (A) are the relative amplitude differences between the light-recorded spectra and subsequent dark-recorded spectra at the low-field shoulder (g = 2.0109; field position A in Figure 1); in (B), the data are the relative amplitudes of the second dark-recorded spectra at the low-field shoulder (g = 2.0109); and in (C), the data are the relative amplitudes of the initial dark-recorded spectra at the low-field maximum (g = 2.0070; field position B in Figure 1). The solid lines in (A) and (B) are single-exponential decay curves with half-times of 2.9 and 168 min, respectively; in (C), the solid line is an exponential rise curve $[A_1 - (A_1 - A_0)\exp(-kt)]$, with a half-time of 0.77 min. No corrections were made for the overlap of the C_1^+ and C_2^+ signals with the Y_Z^+ and Y_D^+ signals. The vertical axis of each plot was scaled independently.

≥15-min data points of Figure 3A; however, at these times, significantly greater error is introduced as C_1^+ formation during the EPR measurements becomes maximal. These determined half-times of loss of Y_Z^+ (~2.9 min) and Y_D^+ (~168 min) compare favorably with the half-times (~2.3 and 206–264 min) of the two components describing loss of Mn^{2+} and DPC photooxidations.

In Figure 3C, we plotted the amplitude of the low-field maximum (g = 2.0070) of the initially recorded dark spectra of Figure 1 versus time of photoinhibition in attempts to very roughly estimate the kinetics of C_2^+ (or C_2^{2+}) formation, as determined by the abundance of stable C_2^+ (Car^+) in samples following photoinhibition and storage. The solid line is a calculated rise curve of the form $A - A\exp(-kt)$, with a half-rise time of 0.8 min. Since the dark storage times of the samples were uncontrolled (see first Results section), this estimate is compromised by the variable contribution of nondecayed Y_D^+ to the total amplitude (about one-third to essentially zero for the ≤4- and 120-min samples, respectively). However, the compromise in the estimate may not be extreme based on the following arguments: (1) the half-rise time of C_2^+ was determined mainly by the ≤4-min photoinhibited samples which received minimal differences in dark storage duration; thus, in these samples, the contribution of Y_D^+ to the total signal amplitude was relatively constant; and (2) the quantum yield of C_2^+ formation is likely similar to the low and approximately equivalent quantum yields of Y_D^+ and C_1^+ formation (Buser et al., 1990). Accordingly, the half-rise times of C_2^+, Y_D^+, and C_1^+ would be similar, and the presence of a relatively constant abundance of partially decayed Y_D^+ would have little impact on the estimation of the kinetics of C_2^+ formation. Though the precise kinetics remain to be determined, we note that our estimate of C_2^+ formation ($t_{1/2}$ ~0.8 min) favorably compares with a component ($t_{1/2}$ ~0.6–0.9 min) observed in photoinhibition-induced loss of photoactivation.

The relatively constant amplitude of the low-field maximum recorded in the light at ambient temperature (Figure 1) implies that C_1^+ (Chl^+) is generated more readily as Y_Z^+ and Y_D^+ formations are lost during photoinhibition. Such behavior is consistent with results from studies of the temperature dependence of C_1^+ formation in nonphotoinhibited O_2-evolving PSII, which indicate increasing C_1^+ formation and decreasing $S_2Q_A^-$ formation with diminishing temperatures (de Paula et al., 1985).

Equation 1 interrelates the formation of C_1^+ with the loss of formation of Y_Z^+ and Y_D^+ as a function of time of photoinhibition of NH_2OH-PSII where (a) S equals the total

$$S = A_Z e^{-k_Z t} + A_D e^{-k_D t} + f_{eff}[C_0 + (C_Z - C_0)(1 - e^{-k_Z t}) + (A_C - C_Z)(1 - e^{-k_D t})] \quad (1)$$

number of observed spins, (b) A_Z, A_D, and A_C equal the maximum number of spins per PSII of Y_Z^+, Y_D^+, and C_1^+, respectively, (c) k_Z and k_D are the first-order rate constants for loss of Y_Z^+ and Y_D^+ formation, respectively, (d) C_0 and C_Z equal the maximum number of spins per PSII due to C_1^+ formed during 20-s illumination before (C_0) and after (C_Z) photodamage to Y_Z, (e) f_{eff} is the efficiency with which each C_1^+ spin could be observed with the microwave power used (20 mW), and (f) t is the time of photoinhibition. The first two terms of eq 1 represent the first-order loss of Y_Z^+ and Y_D^+ formation, respectively. The following three terms represent, in order, the amount of C_1^+ formed during measurements of the light-induced EPR signals in nonphotoinhibited membranes, the additional amount of C_1^+ formed during measurements due to lost Y_Z^+, and, finally, the additional amount of C_1^+ formed during measurements due to lost Y_D^+. Equation 1 thus allows predictions of the kinetic changes of Y_Z^+, Y_D^+, and C_1^+ during photoinhibition of NH_2OH-PSII. The precise changes of each of these species are otherwise extremely difficult to evaluate from the data of Figure 1 for the following reasons: (1) the "Y_D^+" signal includes contributions from C_2^+ and any stable C_1^+; (2) the "Y_Z^+" signal includes contributions from C_1^+; and (3) there is no known explicit relationship between C_1^+ formation with loss of Y_Z^+/Y_D^+ formation.

Accordingly, we evaluated the total light-induced spins per PSII in each of the sets of traces shown in Figure 1 by double integration of the light-recorded trace, assuming a linear base line. The similarly evaluated Y_D^+ signal observed with nonphotoinhibited (t = 0) membranes was equated with 1 spin per PSII. Figure 4 (circles) shows a plot of the total light-induced spins per PSII versus time of photoinhibition. The solid line shown through the circles was obtained by fitting the data to eq 1 using a nonlinear least-squares analysis [Levenborg–Marquardt algorithm (Press et al., 1988)] to obtain the best fit. The best-fit parameters (see Figure 4 legend) suggest (1) the abundance of C_1, like Y_Z and Y_D, is ~1 per PSII, (2) the rate of light-induced C_1^+ formation at ambient temperature increases as Y_Z and Y_D become photodamaged during photoinhibition, and (3) maximum C_1^+ can be seen after 20-s illumination only after abolishing Y_Z and Y_D donation to P_{680}^+. These interrelations between the predicted light-induced abundances of C_1^+, Y_Z^+, and Y_D^+ are also

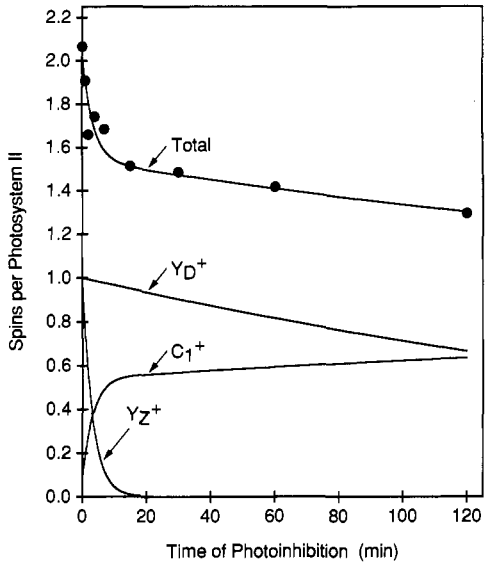

FIGURE 4: Total number of spins per PSII reaction center, and the calculated abundances of Y_Z^+, Y_D^+, and C_1^+ in the light-recorded EPR spectra (20-s illumination), as a function of the time of photoinhibition. The data (circles) are the double integrals of the light-measured spectra in Figure 1, expressed as spins, determined as described in the text. The solid lines (C_1^+, Y_Z^+, and Y_D^+) are calculated according to the individual terms in eq 1, as described in the text, with the following parameter values determined from a best fit of eq 1 to the data (see the text for definitions): A_Z and A_D are 1.0; k_Z = 0.3081 min^{-1}; k_D = 0.0034 min^{-1}; $f_{eff}A_C$ = 0.821; $f_{eff}C_0$ = 0.065; and $f_{eff}C_Z$ = 0.542. The curve marked "total" is the sum of the other three curves.

shown in Figure 4. The sum of the C_1^+, Y_Z^+, and Y_D^+ contributions shown in Figure 4 yields the solid line shown through the circles. The half-times for loss of Y_Z^+ formation and loss of Y_D^+ formation obtained by this analysis are 2.25 and 239 min, in excellent agreement with the 2.2–2.3- and 204–264-min half-times obtained from the loss of photoactivation and Mn^{2+} and DPC photooxidations in these same membranes. We thus believe eq 1 adequately describes the change in abundances of EPR-detectable components as a result of photoinhibition.

The data of Figure 1 and Figure 2C–D gave evidence that C_1^+ (Chl^+) decayed rather rapidly. Nevertheless, the number of spins per PSII, following illumination and decay of Y_Z^+, was always in excess of the dark-stable Y_D^+ contribution to the total spins, as calculated from eq 1. Such behavior was particularly apparent following ~7–15 min of photoinhibition, which promotes a large population of C_1^+ and only small loss of Y_D^+ formation (Figures 1 and 3B). This behavior is also apparent in the dark spectra of Figure 1, measured 1 min after illumination: with increasing durations of photoinhibition, the ratio of the amplitude of the low-field shoulder at A versus the amplitude of the low-field maximum at B diminishes. We attribute these excess spins either to some C_2^+ that is regenerated in the brief darkness or to some fraction of the light-generated C_1^+ signal that did not decay totally in 1 min of subsequent darkness.

Effects of Photoinhibition on the Abundance of P_{680}^+ and Its Reduction. The flash-induced transient absorption change at 820 nm gives information about both the percentage of RC's undergoing stable charge separation and the kinetics of P_{680}^+ reduction (Mathis & Vermeglio, 1975). Two main phases of P_{680}^+ reduction have been observed in non-O_2-evolving PSII membranes: a fast (0.2–40 μs) pH-dependent reduction due to $Y_Z \rightarrow P_{680}^+$ electron transfer and a slower (100–200 μs) reduction due to P_{680}^+/Q_A^- charge recombination [e.g., see Conjeaud and Mathis (1980)]. Still slower kinetic components, of minor amplitude, probably reflect modified Q_A^-/P_{680}^+

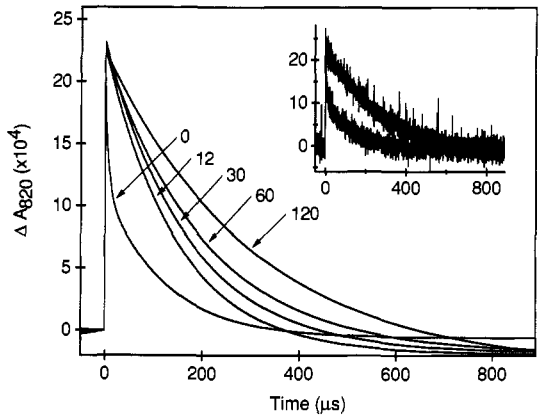

FIGURE 5: The 820-nm absorbance changes associated with the formation and reduction of P_{680}^+, following an actinic laser pulse, in wheat NH_2OH-PSII that had been photoinhibited for various durations. The numbers indicate the minutes of photoinhibition. Each trace is the best fit by an iterative nonlinear least-squares analysis [Levenborg–Marquardt algorithm (Press et al., 1988)] to data resulting from signal-averaging of the first 16 flashes (flash interval = 1 s). The Chl concentration was 80 μg/mL. The ΔA_{820} amplitude corresponds to 1 P_{680}^+/240 Chl, based on an extinction coefficient of 7000 M^{-1} cm^{-1} (Mathis & Paillotin, 1981). The inset shows the raw data for the 0- and 120-min photoinhibited samples.

charge recombination reactions due to different structural states of the reaction center (Gerken et al., 1989). P_{680}^+ reductions by Y_D or by cyt *b*-559 [via C_1^+ (Thompson & Brudvig, 1988)] are both very slow (>5 ms) and would not be seen as distinct decay phases, according to a recent mathematical formulation by Buser et al. (1990).

From the above considerations, photodamage that affects only the redox activity of Y_Z would be manifested as a replacement of the fast 0.2–40-μs component of P_{680}^+ reduction with the slower 100–200-μs P_{680}^+/Q_A^- charge recombination without a decrease in amplitude of the P_{680}^+ absorbance change. On the other hand, photodamage to P_{680}, Pheo, or Q_A, as has been suggested to occur in O_2-evolving systems by several different workers (Cleland et al., 1986; Allakhverdiev et al., 1987; Demeter et al., 1987; Vass et al., 1988; Neale & Melis, 1990; Styring et al., 1990), would result in a diminished amplitude of the P_{680}^+ absorbance change when measured on a microsecond time scale.

In the experiments of Figure 5, we monitored the absorbance changes at 820 nm following the presentation of saturating laser pulses to NH_2OH-PSII that had been previously photoinhibited for various durations (0–120 min). In preliminary measurements, we noticed that while signal-averaging over a large number of pulses the amplitude of the absorbance change steadily decreased (data not shown), presumably due to a real-time photoinhibition of P_{680}^+ formation under the intense near-UV pulses. This type of photoinhibition is different from the weak visible light photoinhibition that is the focus of this study. Consequently, to avoid artifactual contributions from UV-induced damage, we signal-averaged data only from the first 16 flashes (flash frequency was 1 Hz) and then fitted the data to a multiple exponential decay curve. The inset of Figure 5 shows the raw data for the 0- and 120-min photoinhibited samples. All of the data could be fitted adequately to a single- or double-exponential decay, and the best fits thus obtained are shown in Figure 5.

As shown, the amplitude of the flash-induced absorbance change was the same for all samples; thus, we conclude that no photodamage occurs to P_{680}, Pheo, and Q_A even during prolonged photoinhibition of NH_2OH-PSII in weak visible light. However, photoinhibition markedly altered the kinetics

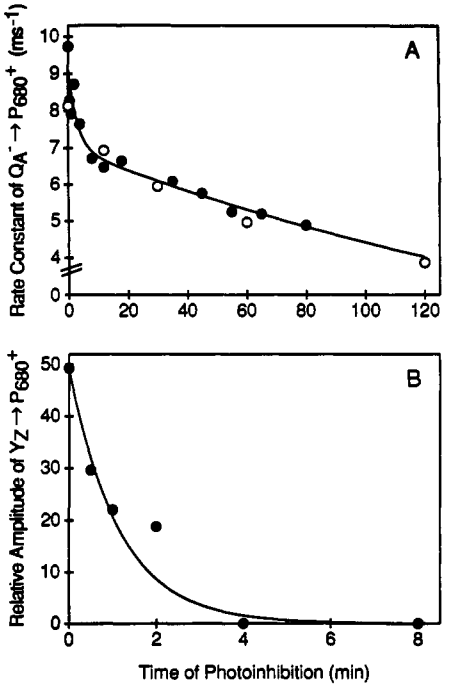

FIGURE 6: First-order rate constant for Q_A^-/P_{680}^+ charge recombination (A) and the extent of Y_Z^+ formation after a flash (B), as a function of the time of photoinhibition. In (A), the rate constants were determined from the 85–180-μs component of P_{680}^+ reduction after a flash (see Figure 5), while in (B) are plotted the relative amplitudes of the 4.5-μs component. The data in (A) are from two separate experiments done on separate days and were determined either in the presence (●) or in the absence (○) of 1 mM ferricyanide. Open circles are from the data of Figure 5. The solid line in (A) is a biphasic curve with half-times and amplitudes, respectively, of 2.2 min and 23.6%, and 150 min and 76.4%; the solid line in (B) is monophasic, with a half-time of 0.8 min.

of P_{680}^+ reduction. The nonphotoinhibited ($t = 0$) membranes exhibited distinct biphasic kinetics, with a 4.5-μs component due to reduction of P_{680}^+ by Y_Z, and an 85-μs component, most likely P_{680}^+/Q_A^- charge recombination (Conjeaud & Mathis, 1980; Gerken et al., 1989). In contrast, the 4.5-μs component was absent in all samples photoinhibited for ≥12 min, consistent with a rapid photodamage affecting the redox activity of Y_Z. After photoinhibition times ≥12 min, the reduction of P_{680}^+ was monophasic, with a half-time that slowly increased with increasing durations of photoinhibition, from a value of 100 μs after 12 min to a value of 180 μs after 120 min. In Figure 6A, the first-order rate constant for P_{680}^+/Q_A^- charge recombination is plotted as a function of the time of photoinhibition. Shown are data from Figure 5 (open circles), along with additional data collected from another preparation (closed circles). The data yield a biphasic curve with half-times of 2.2 and 150 min (solid line), in good agreement with the half-times for loss of Y_Z^+ and Y_D^+ formation, respectively. Apparently, the photodamage affecting formation of Y_Z^+ and Y_D^+ in the near vicinity of P_{680}^+ indirectly modifies the P_{680}^+/Q_A^- charge recombination reaction.

In Figure 6B, the amplitude of the 4.5-μs component, which reflects the extent of Y_Z^+ formation after a single flash, is shown as a function of the time of photoinhibition. The data indicate a half-time of loss of 0.8 min (solid line). This is faster than the loss of Y_Z^+ formed in continuous light, as shown here (Figures 3A and 4) and as deduced from the rate of loss of electron donor photooxidations (Blubaugh & Cheniae, 1990b). It correlates well, however, with the appearance of the C_2^+ radical (Figure 3C). This can be explained by a large decrease in the rate constant for $Y_Z \rightarrow P_{680}^+$ electron transfer in RC's that form C_2^+. For example, if C_2^+ is close to Y_Z, it could electrostatically impair the transfer of an electron from Y_Z to P_{680}^+. Y_Z^+ formation in such RC's would occur with low quantum yield, due to competition with the Q_A^-/P_{680}^+ back-reaction, but would be observed in full abundance under multiple-turnover conditions (Figure 1).

Photoinhibition Effects on the Yield of Flash-Induced Chl a Variable Fluorescence. Relevance of C_1^+ and C_2^+ Formation. The yield of flash-induced variable Chl *a* fluorescence reflects the extent of formation of the state P_{680}^+/Q_A^- [for a review, see van Gorkom (1986)]. Any impairment of the reduction of P_{680}^+ results in a low-fluorescent state, due to quenching by P_{680}^+ [e.g., see Butler et al. (1973)] and rapid P_{680}^+/Q_A^- charge recombination. Since P_{680}^+ reduction by Y_D occurs with low quantum yield (Buser et al., 1990), the amplitude of the flash-induced variable Chl *a* fluorescence should decline roughly in parallel with loss of Y_Z during photoinhibition. However, following only 1 min of photoinhibition, a large (~63%) quenching of the variable component of Chl *a* fluorescence was observed, which did not appear to correlate with photodamage to Y_Z (Blubaugh & Cheniae, 1990b). This quenching was largely eliminated by preequilibration of the photoinhibited membranes with NH_2OH or DPC, both electron donors. The C^+ radical observed at cryogenic temperatures, which we equate with C_1^+ (Figure 1), is known to quench Chl *a* fluorescence (Visser & Rijgersberg, 1975) as does a Car^+ (van Gorkom, 1986), which we equate with C_2^+. The formation of C_2^+ (or C_2^{2+}) and possibly C_1^+ during photoinhibition of NH_2OH-PSII is rapid ($t_{1/2}$ ~0.8 min, Figure 3C), and C_2^+ and possibly a fraction of C_1^+ are stable in the absence of electron donors. Accordingly, we determined the effects of short-term photoinhibition regimes on the amplitude of flash-induced variable Chl *a* fluorescence measured in the presence of DCMU and in the absence or presence of an electron donor (DPC) in efforts to determine whether formation of C_1^+/C_2^+ and the fluorescence quencher were kinetically correlated and reducible by DPC.

In the absence of postaddition of DPC to photoinhibited membranes (closed circles), the data of Figure 7 reveal a rapid ($t_{1/2}$ ~0.6 min) kinetic component correlated with loss of ~60% of the fluorescence yield. This half-time is similar to the half-time of formation of C_2^+ (Figure 3C) and is 3–4 times faster than the half-time of photodamage to Y_Z^+ formation (Figures 3A and 4). The remaining fluorescence yield was lost somewhat slowly ($t_{1/2}$ ~10 min), compared to the usual rate of loss of Y_Z. This behavior is attributed to a certain probability of $Y_D \rightarrow P_{680}^+$ occurring after a flash. As shown by the open circles of Figure 7, the 0.6-min component of photoinhibition was not detectable with photoinhibited membranes which were postincubated with 1 mM DPC prior to the fluorescence measurements. We therefore equate the formation of the quencher of variable fluorescence with formation of C_2^+ (or C_2^{2+}) and conclude that DPC reduces it.

Other chemical reductants, all exogenous donors to PSII, were even more effective than DPC for restoring the quenched fluorescence. Shown in Figure 8 are the concentration dependences of NH_2OH, NH_2NH_2, DPC, and Mn^{2+} for abolishing the fluorescence quencher formed during a 3-min photoinhibition treatment. In this particular experiment, the flash-induced fluorescence amplitude was diminished by ~90% after 3 min of photoinhibition. As shown, increasing concentrations of the reductants led to increasing amplitudes of variable Chl *a* fluorescence until ultimately all but ~30% of the diminished amplitude was restored, an amount we attribute to photodamage to Y_Z. The data of Figure 8 therefore indicate

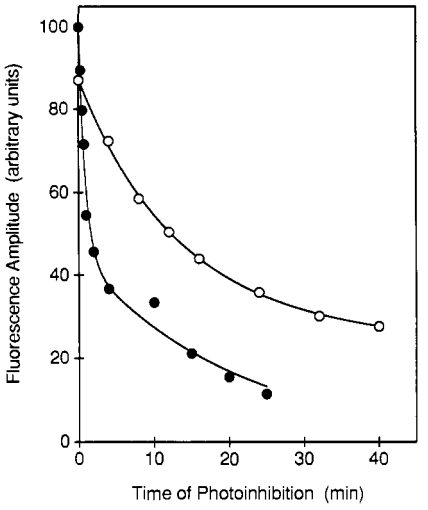

FIGURE 7: Relative amplitude of the variable Chl *a* fluorescence induced by a flash, as a function of the time of photoinhibition. Wheat NH_2OH-PSII membranes were photoinhibited (Materials and Methods) for the time indicated and then immediately dark-adapted for 20 min, during which time (approximately halfway through) DCMU was added in strict darkness to a final concentration of 10 μM; then the flash-induced variable Chl *a* fluorescence was measured as described (Blubaugh & Cheniae, 1990b). The measurements were made either in the absence (●) or in the presence (○) of 1 mM DPC, added in the dark immediately after the photoinhibition treatment. The Chl concentration was 250 μg/mL. The lines are biphasic curves, with the following half-times and amplitudes, respectively: in the absence of DPC, 0.6 min and 56.7%, and 10.4 min and 43.3%; in the presence of DPC, 9.0 min and 68%, and about 250 min and 32%.

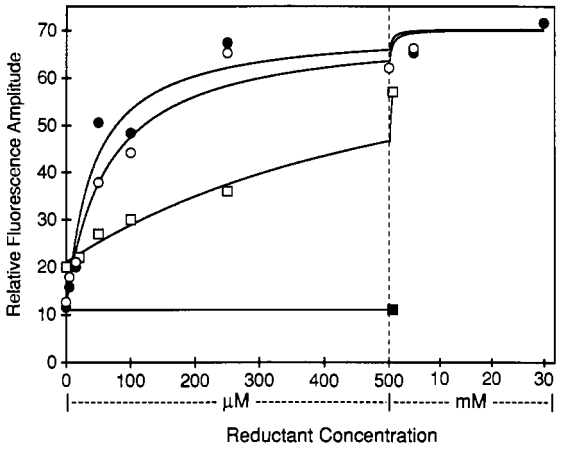

FIGURE 8: Concentration dependence of various reductants on the restoration of the flash-induced variable Chl *a* fluorescence that is lost after 3 min of photoinhibition. Wheat NH_2OH-PSII membranes were photoinhibited for 3 min and then kept on ice in the dark (>1 h). After dark adaptation, NH_2OH (●), NH_2NH_2 (○), DPC (□), or Mn^{2+} (■) was added from 50–100× stock solutions to the indicated final concentrations. The incubation time with the reductant was 10 min in the case of DPC and Mn^{2+}, and <2 min for NH_2OH and NH_2NH_2. The Chl concentration was 250 μg/mL; the data for DPC were collected with a different batch of parent membranes. 100% on the relative scale corresponds to the fluorescence amplitude in nonphotoinhibited control membranes. The solid lines are Michaelis–Menten curves; the following K_m's were obtained: NH_2OH, 39 μM; NH_2NH_2, 65 μM; DPC, 640 μM.

a hierarchy of effectiveness of $NH_2OH \geq NH_2NH_2 >$ DPC $\gg Mn^{2+}$ for the complete reduction of the stable quencher of variable fluorescence. This hierarchy was manifested additionally in the preincubation times required for maximal restoration of the fluorescence amplitude (≤2 min for NH_2OH or NH_2NH_2 and ≥10 min for DPC). Such slow reactivity may reflect restricted access of exogenous reductants to C_2^+. Interestingly, although loss of photoactivation capacity exhibits

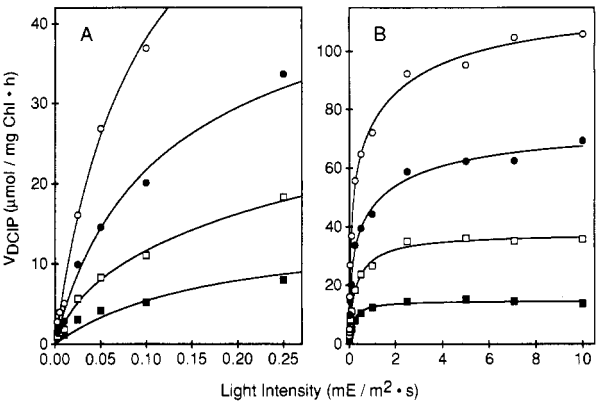

FIGURE 9: Light saturation dependence of Mn^{2+} photooxidation by control and photoinhibited spinach NH_2OH-PSII membranes. Spinach NH_2OH-PSII membranes were photoinhibited for (○) 0, (●) 1, (□) 2, and (■) 5 min, pelleted, and resuspended in buffer, and then rates of Mn^{2+} photooxidation were determined spectrophotometrically as rates of DCIP photoreduction (Blubaugh & Cheniae, 1990b). The assay mixture in buffer A contained 50 μM DCIP, 1 μM $MnCl_2$, 3.0 mM H_2O_2, and NH_2OH-PSII membranes equivalent to 20 μg of Chl/mL. Neutral density filters were used to vary the light intensity. The same data are shown to different scales in (A) and (B).

a kinetic component with the same half-time as formation of the quencher, a 5-min incubation with 250 μM NH_2OH, followed by extensive washing, did not restore any of the lost capacity for photoactivation, though it did restore most of the lost fluorescence amplitude (data not shown).

Effects of Photoinhibition on the Relationship of Light Intensity vs Rate of Mn^{2+} Photooxidation. A number of photoinhibition studies made with O_2-evolving cells or chloroplasts have given evidence that the light-limited rates of electron transfers are inhibited sooner and more extensively than inhibition of the light-saturated rates [for a review, see Powles (1984)]. This behavior might indicate that the primary event of photoinhibition is a decrease in the transfer of excitation energy from the antenna complex to the reaction center. The formation of Chl^+ has been suggested to indicate this presumed primary event, and then to cause secondary photodamage to reaction center components (Thompson & Brudvig, 1988). The data in the preceding sections showed that among the early events in photoinhibition of NH_2OH-PSII were the rapid formation of C_1^+/C_2^+, the quenching of Chl *a* variable fluorescence, and the slowing of P_{680}^+ reduction by Y_Z, followed by the apparent loss of Y_Z^+ and Y_D^+ formation. In the experiments of Figure 9, we asked if a decoupling of the antenna from the reaction center complex might also occur as an early event (Zhao & Brand, 1988, 1989; Hayden et al., 1986).

Accordingly, spinach NH_2OH-PSII membranes were photoinhibited for 0, 1, 2, and 5 min; then rates of Mn^{2+} photooxidation in the presence of 3 mM H_2O_2 were determined over a 4000-fold range of light intensity. Whereas 3 mM H_2O_2 itself was an ineffective exogenous donor, its addition markedly increased the quantum yield, as well as the rates, of Mn^{2+} photooxidation in saturating light, and Mn^{2+} photooxidation rates of only 1–2 μmol (mg of Chl)$^{-1}$ h^{-1} could be measured with high reproducibility. Relative to the control, the 1-, 2-, and 5-min photoinhibition regimes diminished the relative quantum efficiency by 47, 70, and 88%, respectively, determined from the initial slopes of the light intensity curves (Figure 9A), while the rates measured with 20 μg of Chl/mL in saturating light (Figure 9B) decreased 37, 65, and 86%, respectively. (Similar percentage decreases were obtained by using only 0.8 μg of Chl/mL.) The nearly proportionate

Scheme I: Pathways of Electron Flow in NH_2OH-PSII

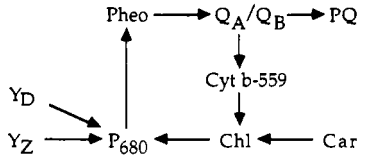

decreases by photoinhibition of the light-limited and light-saturated rates of Mn^{2+} photooxidation lead us to conclude that no gross decoupling of the antenna from the reaction center complex occurs during ≤5-min photoinhibition of spinach NH_2OH-PSII membranes. This conclusion is also consistent with the full abundance of P_{680}^+ observed in a single flash (Figure 5).

Discussion

The data presented here reveal a complex sequence of photodamages which occur during photoinhibition of non-O_2-evolving PSII membranes (NH_2OH-PSII). These photodamaging effects will be discussed with reference to Scheme I. The order of events that we observe is as follows: (1) the appearance of a stable quencher of variable Chl *a* fluorescence, correlated with a dark-stable radical that has EPR characteristics of a Car^+ (Grant et al., 1988), and a slowing of the $Y_Z \rightarrow P_{680}^+$ electron transfer, all with similar half-times of ~0.8 min; (2) the loss of Y_Z^+ formation ($t_{1/2}$ ~2.3 min); and (3) the loss of Y_D^+ formation ($t_{1/2}$ = 3–4 h). No loss of P_{680}^+/Q_A^- charge separation occurs, and, moreover, no loss of formation of a radical, typical for Chl^+ [see Visser et al. (1977) and de Paula et al. (1985)], is observed even with prolonged (120 min) photoinhibition. The latter result suggests that the Q_A–Q_B locus also does not suffer photodamage, since electron transport occurs unimpaired with Chl as donor. We therefore attribute the loss of Y_Z^+ and Y_D^+ formation either directly to these specific tyrosyl residues or to the amino acid residues in their immediate vicinities such that the Y_Z and Y_D redox activities are abolished.

We suggest that events 1 and 2 reflect one process in which the initial slowing of the $Y_Z \rightarrow P_{680}^+$ reaction increases the quantum yield of formation of Chl^+, which in turn oxidizes Car, followed by a further slowing of Y_Z to P_{680}^+. (We cannot rule out that Chl and Car are oxidized in parallel.) A similar process may account for event 3. We propose that the greater susceptibility of Y_Z to photodamage, compared to Y_D, is causally related to the higher quantum efficiency of Y_Z^+ formation, relative to Y_D^+ (Buser et al., 1990), and that P_{680}^+ is the causative agent for the photodamages. This contrasts to Thompson and Brudvig's (1988) suggestion that formation of Chl^+ is the primary causative event in photoinhibition, though it agrees with their hypothesis that Chl^+ formation is an early event. No evidence was found to support the hypothesis that Chl^+ formation causes a gross decoupling of the antenna complex from the reaction center (Figure 9).

The maximum quantum yield of Chl^+ formation is dependent on the loss of electron donation from Y_Z^+ and Y_D^+ to P_{680}^+ (Figure 4). Most of the resulting Chl^+ is reduced rapidly, presumably by cyt *b*-559 (Thompson & Brudvig, 1988). Tamura and Cheniae (1987) showed that some cyt *b*-559 is converted to its very low redox potential form during photoinhibition. This would be expected to remove cyt *b*-559 in some centers from the redox loop shown in Scheme I and result in an increased stability of some fraction of the total Chl^+. This prediction is consistent with the observation in Figure 1 that the ratio of low-field maximum to low-field shoulder in the dark-after-light EPR spectra increases with increasing durations of photoinhibition.

The observed quencher of Chl *a* variable fluorescence conceivably reflects formation of Chl^+, Car^+ (van Gorkom, 1986), and possibly Car^{2+}. The quencher was dark-stable but chemically reducible by some exogenous electron donors, excluding Mn^{2+}. Only Chl^+ (maximally, ≤1 spin/PSII) was observed during the light-recorded EPR spectra; nevertheless, Car^+ was observed following prolonged dark storage of the photoinhibited membranes (>5 months at −80 °C and ~10 h at 4 °C). These observations are explained by rapid formation of EPR-silent Car^{2+} which then slowly gives rise to some Car^+. The oxidation of β-carotene to a dication and the stability of its monocation at room temperature ($t_{1/2}$ of several minutes) have been demonstrated in some organic solvents (Grant et al., 1988). Although we tentatively indentify C_2^+ as Car^+ and C_1^+ as Chl^+, we cannot exclude the hypothesis that either or both species may be a modified Y_Z^+ and/or Y_D^+ or Y_Z^+ and/or Y_D^+ in a modified environment (Tso et al., 1990; Baumgarten et al., 1990). However, we favor our assignments, as these would account for the observed quenching of Chl *a* fluorescence.

The appearance of the quencher ($t_{1/2}$ = 0.6 min) and the slowing of the $Y_Z \rightarrow P_{680}^+$ reaction ($t_{1/2}$ ~0.8 min) are also correlated with a loss ($t_{1/2}$ ~0.8 min) of about 50% of the capacity for photoactivation (Blubaugh & Cheniae, 1990b). This loss is proposed to be a result of further decrease of the already low quantum yield of the Y_Z^+-driven photoactivation process, due to increased P_{680}^+/Q_A^- back-reactions (Figure 6B). The somewhat faster decrease of light-limited rates compared to light-saturated rates of O_2-evolution during photoinhibition of O_2-evolving cells and chloroplasts [reviewed by Powles (1984)] can be similarly explained.

The half-times of photodamage causing loss of Y_Z^+ and Y_D^+ formation correspond closely to the loss of high quantum yield photooxidations of electron donors (Mn^{2+}, DPC, and I^-) through site 1 ($t_{1/2}$ ~2–3 min) and the loss of their low quantum yield photooxidations through site 2 ($t_{1/2}$ ~1–4 h) (Blubaugh & Cheniae, 1990b). We therefore associate site 1 with Y_Z and site 2 with Y_D. Whereas reduction of Y_Z^+ by exogenous donors, including Mn^{2+}, is well documented, some literature states that the reduction of Y_D^+ by Mn^{2+} does not occur (Hoganson et al., 1989; Miller & Brudvig, 1990). Thus, definitive proof for the identification of site 2 is still lacking.

The observed loss of Y_Z^+ and Y_D^+ formation also offers an explanation for the parallel loss of electron donor photooxidations and proteolysis of D_1 during short-term photoinhibition of Cl^--depleted chloroplasts (Jergerschold et al., 1990), as well as the necessity for synthesis and assembly of both D_1 and D_2 polypeptides for the recovery of PSII functions following extensive photoinhibition of NH_2OH-treated leaves (Callahan et al., 1986).

These interpretations of the early events in the photoinhibition of non-O_2-evolving membranes are relevant to the results of Klimov et al. (1990) showing that photoinhibition caused rapid photooxidation of 2–3 Car's per PSII RC, in parallel with a loss of capacity for photoactivation. Our results contrast, however, with their interpretation that Y_Z^+ and Y_D^+ formation is unimpaired. We note that their EPR data show a very small low-field shoulder in both control and photoinhibited samples, suggesting that some photoinhibition may already have occurred to the controls.

An impairment of Y_Z^+ and Y_D^+ formation and specific quenching of the variable Chl *a* fluorescence has also been reported following UV-induced photodamage to O_2-evolving PSII membranes, chloroplasts, and leaves (Yerkes et al., 1990). Finally, our interpretations of the effects of non-UV, visible

light photoinhibition may be relevant to the sequence of damages in O_2-evolving cells and chloroplasts exposed to very high light intensities. The somewhat faster loss of light-limited rates of electron transport, compared to light-saturated rates, and the rapid fluorescence quenching that precede loss of electron transport [reviewed by Powles (1984) and Kyle (1987)], a Chl^+-like signal evident in the EPR spectrum after photoinhibition (Ohad et al., 1990), and the loss of the D_1 followed by D_2 proteins (Virgin et al., 1988; Jergerschold et al., 1990; Hundal et al., 1990b) are all consistent with the scheme presented. Possibly, at high light intensities, the internal pH of the lumen becomes sufficiently acidic to decrease the $S_3 \rightarrow S_4$ transition of the water-oxidizing complex (Wraight et al., 1972; Bowes & Crofts, 1981) and to slow $Y_Z \rightarrow P_{680}^+$ [e.g., see Conjeaud and Mathis (1990)], resulting in increased steady-state populations of Y_Z^+ and P_{680}^+ and increased susceptibility to photodamage of the oxidizing side of PSII.

ACKNOWLEDGMENTS

We thank Iris Deaton for her help in preparation of the manuscript. We also are grateful to Mohamed El-Deeb for his technical assistance with the EPR measurements.

Registry No. P_{680}, 53808-91-6; O_2, 7782-44-7; Tyr, 60-18-4.

REFERENCES

Adir, N., Schochat, S., & Ohad, I. (1990) *J. Biol. Chem. 265*, 12563–12568.

Allakhverdiev, S. I., Setlikova, E., Klimov, V. V., & Setlik, I. (1987) *FEBS Lett. 226*, 186–190.

Arntz, B., & Trebst, A. (1986) *FEBS Lett. 194*, 43–49.

Babcock, G. T. (1987) in *Photosynthesis* (Amesz, J., Ed.) pp 125–158, Elsevier, Amsterdam.

Babcock, G. T., Barry, B. A., Debus, R. J., Hoganson, C. W., Atamian, M., McIntosh, L., Sithole, I., & Yocum, C. F. (1989) *Biochemistry 28*, 9557–9565.

Baumgarten, M., Philo, J. S., & Dismukes, G. C. (1990) *Biochemistry 29*, 10814–10822.

Becker, D. W., Callahan, F. E., & Cheniae, G. M. (1985) *FEBS Lett. 192*, 209–214.

Becker, D. W., Callahan, F. E., & Cheniae, G. M. (1987) in *Progress in Photosynthesis Research* (Biggins, J., Ed.) Vol. IV, pp 31–34, Martinus Nijhoff, Dordrecht, The Netherlands.

Blubaugh, D. J., & Cheniae, G. M. (1990a) in *Current Research in Photosynthesis* (Baltscheffsky, M., Ed.) Vol. I, pp 503–506, Kluwer Academic Publishers, Dordrecht, The Netherlands.

Blubaugh, D. J., & Cheniae, G. M. (1990b) *Biochemistry 29*, 5109–5118.

Bock, C. H., Gerken, S., Stehlik, D., & Witt, H. T. (1988) *FEBS Lett. 277*, 141–146.

Bowes, J. M., & Crofts, A. R. (1981) *Biochim. Biophys. Acta 637*, 464–472.

Buser, C. A., Thompson, L. K., Diner, B. A., & Brudvig, G. W. (1990) *Biochemistry 29*, 8977–8985.

Butler, W. L., Visser, J. W. M., & Simons, H. L. (1973) *Biochim. Biophys. Acta 325*, 539–545.

Callahan, F. E., & Cheniae, G. M. (1985) *Plant Physiol. 79*, 777–786.

Callahan, F. E., Becker, D. W., & Cheniae, G. M. (1986) *Plant Physiol. 82*, 261–268.

Cleland, R. E., Melis, A., & Neale, P. J. (1986) *Photosynth. Res. 9*, 79–88.

Conjeaud, H., & Mathis, P. (1980) *Biochim. Biophys. Acta 590*, 353–359.

Critchley, C. (1988) *Photosynth. Res. 19*, 265–276.

de Paula, J. C., Innes, J. B., & Brudvig, G. W. (1985) *Biochemistry 24*, 8114–8120.

Dekker, J. P., van Gorkom, H. J., Brok, M., & Ouwehand, L. (1984) *Biochim. Biophys. Acta 764*, 301–309.

Demeter, S., Neale, P. J., & Melis, A. (1987) *FEBS Lett. 214*, 370–374.

Gerken, S., Dekker, J. P., Schlodder, E., & Witt, H. T. (1989) *Biochim. Biophys. Acta 977*, 52–61.

Grant, J. L., Kramer, V. J., Ding, R., & Kispert, L. D. (1988) *J. Am. Chem. Soc. 110*, 2151–2157.

Hansson, O., & Wydrzynski, T. (1990) *Photosynth. Res. 23*, 131–162.

Hayden, D. B., Baker, N. R., Percival, M. P., & Beckwith, P. B. (1986) *Biochim. Biophys. Acta 851*, 86–92.

Hoganson, C. W., Ghanotakis, D. F., Babcock, G. T., & Yocum, C. F. (1989) *Photosynth. Res. 22*, 285–293.

Hundal, T., Aro, E.-M., Carlberg, I., & Andersson, B. (1990a) *FEBS Lett. 267*, 203–206.

Hundal, T., Virgin, I., Styring, S., & Andersson, B. (1990b) *Biochim. Biophys. Acta 1017*, 235–241.

Jegerschold, C., Virgin, I., & Styring, S. (1990) *Biochemistry 29*, 6179–6186.

Klimov, V. V., Shafiev, M. A., & Allakhverdiev, S. I. (1990) *Photosynth. Res. 23*, 59–65.

Krause, G. H., Koster, S., & Wong, S. C. (1985) *Planta 165*, 430–438.

Kyle, D. J. (1987) in *Photoinhibition* (Kyle, D. J., Osmond, C. B., & Arntzen, C. J., Eds.) pp 197–226, Elsevier, New York.

Kyle, D. J., Ohad, I., & Arntzen, C. J. (1984) *Proc. Natl. Acad. Sci. U.S.A. 81*, 4070–4074.

MacKinney, G. (1941) *J. Biol. Chem. 140*, 315–322.

Mathis, P., & Vermeglio, A. (1975) *Biochim. Biophys. Acta 396*, 371–381.

Mathis, P., & Paillotin, G. (1981) in *The Biochemistry of Plants: A Comprehensive Treatise* (Stumpf, P. K., & Conn, E. E., Eds.) Vol. 8, pp 97–161, Academic Press, New York.

Mathis, P., & Rutherford, A. W. (1987) in *Photosynthesis* (Amesz, J., Ed.) pp 63–96, Elsevier, Amsterdam.

Mattoo, A. K., Hoffman-Falk, H., Marder, J. B., & Edelman, M. (1984) *Proc. Natl. Acad. Sci. U.S.A. 81*, 1380–1384.

Miller, A.-F., & Brudvig, G. W. (1990) *Biochemistry 29*, 1385–1392.

Neale, P. J., & Melis, A. (1990) *Plant Physiol. 92*, 1196–1204.

Nugent, J. H. A., Evans, M. C. W., & Diner, B. (1982) *Biochim. Biophys. Acta 682*, 106–114.

Ohad, I., Kyle, D. J., & Arntzen, C. J. (1984) *J. Cell Biol. 99*, 481–485.

Ohad, I., Koike, H., Schochat, S., & Inoue, Y. (1988) *Biochim. Biophys. Acta 933*, 288–298.

Ohad, I., Adir, N., Koike, H., Kyle, D. J., & Inoue, Y. (1990) *J. Biol. Chem. 265*, 1972–1979.

Ono, T.-A., Kajikawa, H., & Inoue, Y. (1986) *Plant Physiol. 80*, 85–90.

Powles, S. B. (1984) *Annu. Rev. Plant Physiol. 35*, 15–44.

Press, W. H., Flannery, B. P., Teukolsky, S. A., & Vetterling, W. T. (1988) *Numerical Recipes in C: The Art of Scientific Computing*, Cambridge University Press, New York.

Satoh, K., & Fork, D. C. (1982) *Plant Physiol. 70*, 1004–1008.

Schenck, C. C., Diner, B., Mathis, P., & Satoh, K. (1982) *Biochim. Biophys. Acta 680*, 216–227.

Styring, S., Virgin, I., Ehrenberg, A., & Andersson, B. (1990) *Biochim. Biophys. Acta 1015*, 269–278.

Tamura, N., & Cheniae, G. M. (1987) *Biochim. Biophys. Acta 890*, 179–194.
Theg, S. M., Filar, L. J., & Dilley, R. A. (1986) *Biochim. Biophys. Acta 849*, 104–111.
Thompson, L. K., & Brudvig, G. W. (1988) *Biochemistry 27*, 6653–6658.
Trebst, A. (1962) *Z. Naturforsch. 17B*, 660–663.
Trebst, A., Depka, B., & Kipper, M. (1990) in *Current Research in Photosynthesis* (Baltscheffsky, M., Ed.) Vol. I, pp 217–223, Kluwer Academic Publishers, Dordrecht.
Tso, J., Petrouleas, V., & Dismukes, G. C. (1990) *Biochemistry 29*, 7759–7767.
van Gorkom, H. J. (1986) in *Light Emission by Plants and Bacteria* (Govindjee, Amesz, J., & Fork, D. C., Eds.) pp 267–289, Academic Press, New York.
Vass, I., Mohanty, N., & Demeter, S. (1988) *Z. Naturforsch. 43C*, 871–876.
Vass, I., Deak, Z., Jegerschold, C., & Styring, S. (1990) *Biochim. Biophys. Acta 1018*, 41–46.
Virgin, I., Styring, S., & Andersson, B. (1988) *FEBS Lett. 233*, 408–412.
Virgin, I., Ghanotakis, D., & Andersson, B. (1990) *FEBS Lett. 269*, 45–48.
Visser, J. W. M., & Rijgersberg, C. P. (1975) *Proceedings of the Third International Congress on Photosynthesis* (Avron, M., Ed.) Vol. I, pp 399–408, Elsevier, Amsterdam.
Visser, J. W. M., Rijgersberg, C. P., & Gast, P. (1977) *Biochim. Biophys. Acta 460*, 36–46.
Wraight, C. A., Kraan, G. P. B., & Gerrits, N. M. (1972) *Biochim. Biophys. Acta 283*, 259–267.
Yerkes, C. T., Kramer, D. M., Fenton, J. M., & Crofts, A. R. (1990) in *Current Research in Photosynthesis* (Baltscheffsky, M., Ed.) Vol. II, pp 381–384, Kluwer Academic Publishers, Dordrecht, The Netherlands.
Zhao, J., & Brand, J. J. (1988) *Arch. Biochem. Biophys. 264*, 657–664.
Zhao, J., & Brand, J. J. (1989) *Plant Physiol. 91*, 91–100.

Magnetic State of the a_3 Center of Cytochrome *c* Oxidase and Some of Its Derivatives†

Zexia K. Barnes*
Department of Physical Sciences, Morehead State University, Morehead, Kentucky 40351-1689
Gerald T. Babcock and James L. Dye
Department of Chemistry, Michigan State University, East Lansing, Michigan 48824-1322
Received November 5, 1990; Revised Manuscript Received May 17, 1991

ABSTRACT: The temperature dependence of the magnetic susceptibility was used to investigate the nature of the coupling between cytochrome a_3 and Cu_B in resting and oxidized cyanide- and formate-bound cytochrome oxidase. Resting and formate-bound enzymes were found to have strong antiferromagnetic coupling with an $S = {}^5/_2$ cytochrome a_3, results that were independent of the dispersing detergent and the enzyme isolation method. The cyanide-bound enzyme was heterogeneous, with a minor fraction showing intermediate strength antiferromagnetic coupling. The magnitude of this coupling was independent of the enzyme isolation method and depended moderately on the identity of the dispersing detergent. The major fraction of the cyanide-bound enzyme had a lowest energy state of $M_s = 0$. The coupling constant for this fraction did not depend on the isolation technique or on the identity of the dispersing detergent. The use of glucose–glucose oxidase to deoxygenate samples influenced the susceptibility behavior of some preparations of both the resting and formate-bound enzymes, with results indicating an $S = {}^3/_2$ cytochrome a_3 in the resting enzyme samples. Retention of a 417-nm Soret band for formate-bound enzyme concomitant with peroxide-induced changes in susceptibility behavior indicates different sites of enzyme interactions for the formate ion and hydrogen peroxide.

It was suggested over 20 years ago (Van Gelder & Beinertt, 1969) that the lack of EPR signals from cytochrome a_3 and Cu_B in oxidized, resting cytochrome oxidase is due to their magnetic coupling but the nature of that coupling is still unresolved [for general reviews of cytochrome oxidase, see Wikstrom et al. (1981), Naqui et al. (1986), Scott (1989), and Chan and Li (1990)]. Both ferromagnetic coupling (Thomson et al., 1981; Kent et al., 1982) and antiferromagnetic coupling (Tweedle et al., 1978) have been reported for the resting or cyanide-bound enzyme as a result of MCD, Mössbauer, and magnetic susceptibility measurements. As with much of the work done with cytochrome oxidase, the various experiments were carried out by using enzyme isolated with different methods, different dispersing detergents, or different solvents. In addition, oxygen was removed from the magnetic susceptibility samples by addition of glucose oxidase and glucose, a technique that produces peroxide that can bind to the enzyme.

The enzyme isolation method used affects the reduction and ligand-binding properties of cytochrome oxidase (Jones et al., 1983; Naqui et al., 1984; Halaka et al., 1984; Baker et al., 1987; Hartzell et al., 1988), and the identity of the dispersing detergent can affect the enzyme activity (Rosevear et al., 1980;

† This investigation was partially supported by National Institutes of Health Grant GM25480 (to G.T.B.).

0006-2960/91/0430-7597$02.50/0